Fourier Transform Infrared Spectroscopic Studies of the Secondary Structure of Spectrin under Different Ionic Strengths†

C. C. LaBrake,‡ L. Wang,§ T. A. Keiderling,§ and L. W.-M. Fung*,‡

Department of Chemistry, Loyola University of Chicago, Chicago, Illinois 60626, and Department of Chemistry, University of Illinois at Chicago, Chicago, Illinois 60680

Received May 14, 1993; Revised Manuscript Received July 12, 1993®

ABSTRACT: Spectrin, a highly dynamic skeletal membrane protein, plays an important role in maintaining the disk biconcave shape of the human erythrocyte. The sequence of spectrin is mostly composed of repeating segments of 106 amino acids which have been proposed to form unique structural domains. Electronic and vibrational circular dichroism and Fourier transform infrared (FTIR) spectroscopy were used as complementary techniques to study the secondary structure of spectrin. The amide I and II regions of the FTIR absorbance spectra were analyzed using partial least-squares analysis. The secondary structure of spectrin under physiological buffer conditions was estimated to be about 70% α-helix, 10% β-sheet, and 20% other. We believe that this is the first detailed experimental evidence of significant β-sheet content in spectrin secondary structure. The antiparallel β-sheet SH3 domain in the center of the α-subunit in spectrin accounts for only about 1.5% of the total amino acid residues in the dimer. Hydrodynamic studies have shown spectrin to be sensitive to changes in ionic strength and to addition of denaturing agents. Our FTIR results showed that the secondary structure of spectrin treated with detergent or NaOH changed by 10–20%. The Stokes radii of the spectrin samples used for FTIR measurements were found to vary as a function of the ionic strength, but their secondary structures did not change as a function of ionic strength. These results indicate that while the overall hydrodynamic dimension of spectrin depends on the medium ionic strength, the secondary structure remains essentially constant. Thus, the salt-induced contraction and expansion of erythrocyte skeleton cannot be explained by changes in spectrin secondary structures, either in contents or in α-helical lengths.

Human erythrocyte spectrin is the major component in a two-dimensional skeletal network on the cytoplasmic side of the erythrocyte membrane and plays a dominant role in determining the mechanical properties, *e.g.*, elasticity and deformability, of the erythrocyte. Membrane skeletons extracted from erythrocytes can expand or shrink with changing ionic strength, pH, temperature, or concentration of a denaturant (Johnson *et al.*, 1980; Lange *et al.*, 1982; Vertessy & Steck, 1989; Svoboda *et al.*, 1992). Light-scattering and synchrotron-based small-angle X-ray-scattering experiments of isolated membrane skeletons suggest that the skeletal expansion in low salt (50 mM Na^+) is due to the conversion of spectrin tetramers to dimers (Schmidt *et al.*, 1993).

Spectrin is comprised of α- and β-subunits associated side-to-side to form a flexible heterodimer, which was reported to have a length of approximately 100 nm (Shotton *et al.*, 1979). This dimension agrees well with the contour length measured in the skeleton in low salt (Schmidt *et al.*, 1993). No information on the dimension of spectrin dimers under physiological salt (high salt) condition was reported. The αβ-dimers form end-to-end association to give tetramers. Circular dichroism (CD) secondary structural studies suggest high α-helix content in spectrin (Ralston, 1978; Calvert *et al.*, 1980). Amino acid (Speicher *et al.*, 1983; Sahr *et al.*, 1990) and cDNA (Winkelmann *et al.*, 1988) sequence analyses reveal that both the α- and β-subunits of spectrin are comprised of largely repetitive units of homologous sequences of 106 amino acid residues. The 106-residue segments have been proposed to fold into a simple triple-helical structure (Speicher *et al.*, 1983). Variations to this simple model were suggested later, with some of these models including some β-sheet features (Davison *et al.*, 1989; Dubreuil *et al.*, 1989; Xu *et al.*, 1990; Speicher *et al.*, 1993). The triple-helical model has also been developed to give a left-handed, coiled-coil structure stabilized by maximum ion pairing between the three helices in the 106-residue segments (Parry *et al.*, 1992). In addition to the 106-residue segments, spectrin also includes a small region of antiparallel β-barrel structure in the center of the α-chain (Musacchio *et al.*, 1992; Yu *et al.*, 1992). An EF-hand structure at the C-terminal end of the α-chain has also been suggested (Speicher *et al.*, 1992).

Studies with various physical methods have shown spectrin to be a highly dynamic molecule with multiple classes of internal, segmental motions (Mikkelsen & Elgsaeter, 1978; Fung & Johnson, 1983; Mikkelsen *et al.*, 1984; Fung *et al.*, 1986, 1989; Clague *et al.*, 1990; Budzynski *et al.*, 1992). Nuclear magnetic resonance (NMR)[1] studies of spectrin under different salt conditions suggest different amounts of segmental motions under these salt conditions (Fung *et al.*, 1986, 1989; unpublished results). Spin-label electron paramagnetic resonance (EPR) studies of spectrin reveal the conversion of a weakly immobilized component to a strongly immobilized component upon increasing salt concentration to 150 mM NaCl (Fung & Johnson, 1983; unpublished results). Hydrodynamic studies of spectrin have shown that the size or dimension of spectrin appears to vary as a function of ionic

† This research was supported in part by grants from the NIH (R01HL38361 to L.W.-M.F. and R01GM30147 to T.A.K.) and by the American Heart Association National Chapter (L.W.-M.F.). C.C.L. is an American Heart Association of Metropolitan Chicago Postdoctoral Research Fellow.

* Author to whom correspondence should be addressed.
‡ Loyola University of Chicago.
§ University of Illinois at Chicago.

® Abstract published in *Advance ACS Abstracts,* September 1, 1993.

0006-2960/93/0432-10296$04.00/0

strength. The elution time of pure spectrin on agarose gels decreases upon decreasing the salt concentration in the spectrin medium (Ralston, 1976). The sedimentation coefficients for both spectrin dimer and spectrin tetramer were lower under low-salt conditions than under high-salt conditions (Brauer *et al.*, 1977; Ralston & Dunbar, 1979). Light scattering experiments have revealed that the radius of gyration of spectrin dimer nearly doubles upon decreasing the ionic strength from 100 to 1 mM NaCl (Elgsaeter, 1978). These hydrodynamic data imply that spectrin molecules increase their dimensions with decreasing ionic strength.

Ralston and Dunbar (1979) have shown that CD data on spectrin suggested a small (3%) difference in α-helix content upon addition of 100 mM NaCl while optical rotary dispersion data revealed no difference in the secondary structure upon NaCl addition. Thus, it is not clear whether the salt-induced changes in spectrin observed in hydrodynamic, NMR, and EPR studies are due to changes in the secondary structure, such as the helix and sheet contents and/or the helical lengths, or a change in the rearrangement of the secondary or tertiary structural elements in spectrin dimers. Therefore, a detailed study of the secondary structure of spectrin under different ionic strengths is warranted.

Recent developments in infrared (IR) spectroscopy using Fourier transform (FT) instrumentation have eliminated the problems of low sensitivity and interfering absorbances by solvents such as water (Surewicz & Mantsch, 1988). Thus, on evaluation of the FTIR spectra in the amide I and II regions of spectrin in aqueous (H_2O) solution of different salt concentrations, we obtain an estimation of the precentage of secondary structural components in spectrin under these conditions. More importantly, these FTIR spectra can be used as a sensitive monitor of conformational change with environmental variation. In addition, the frequency of the amide I absorbance reveals the strength of the H-bonding, and thus provides a means to compare the helix segment lengths in the spectrin backbone under different salt concentrations. We also used electronic and vibrational circular dichroism techniques as complementary techniques to study the secondary structure of spectrin. We found that spectrin did not undergo salt-induced secondary structural changes, either in structural contents or in α-helical lengths, at room temperature in phosphate buffer at pH 7.4.

MATERIALS AND METHODS

Spectrin Preparation. The spectrin dimer preparation was done according to published methods (Ungewickell & Gratzer, 1978; Budzynski *et al.*, 1992), and all steps were carried out at 4 °C unless specified otherwise. Briefly, human red blood cells (RBCs) from the local blood bank were used within 2 weeks of withdrawal. RBCs were washed 3 times with 5 mM sodium phosphate buffer with 150 mM NaCl at pH 8.0 (PBS8), and lysed with 20 volumes of 5 mM phosphate buffer at pH 8.0 (5P8). The membrane ghosts were washed 3 times with the same buffer and 1 time with 0.3 mM phosphate buffer at pH 7.6 (0.3P7.6) before incubation with 2–3 volumes of 0.3P7.6 for 30 min at 37 °C. After incubation, the membranous solution was centrifuged at 400000*g* for 20 min to collect the supernatant containing the spectrin–actin complex. The complex was concentrated to about 1.5 mg/mL, using a molar absorptivity of $\epsilon_{280}^{1\%} = 10.7$ (Marchesi *et al.*, 1969; Clarke, 1971). The spectrin–actin complex was loaded onto a gel filtration column (Sepharose 4B-CL; Pharmacia, Piscataway, NJ) equilibrated with 25 mM Tris, 5 mM EDTA, and 100 mM NaCl at pH 7.6 and eluted at a flow rate of 22 mL/h for about 16 h. The spectrin fractions were pooled and concentrated to about 5–10 mg/mL and dialyzed overnight against either PBS7.4 (same as PBS8 except at pH 7.4) or 5P7.4 (same as 5P8 except at pH 7.4). The spectrin was further concentrated to 35 ± 5 mg/mL.

To prepare denatured spectrin, 10% sodium dodecyl sulfate (SDS) (Bio-Rad, Richmond, CA) in PBS7.4 (50 μL) was added at room temperature to spectrin dimer in PBS7.4 (450 μL at 35 ± 5 mg/mL) to give a final concentration of 1% SDS. The mixture was allowed to equilibrate for about 1 h before the FTIR measurements. A 1% SDS solution in PBS7.4 was used as a blank. Concentrated sodium hydroxide (NaOH) was added to the spectrin dimer in PBS7.4 (35 ± 5 mg/mL) to yield a final NaOH concentration of 2 M. Buffer with 2 M NaOH was used as a blank.

Stokes Radius. To ensure that the spectrin used in FTIR studies exhibited the ionic strength induced hydrodynamic property changes reported in the literature, we followed published methods (Kam *et al.*, 1977) to estimate the Stokes radius (R_s) of spectrin under different ionic strength conditions using a gel filtration column (Sepharose 4B-CL, 81 × 1.5 cm) with a flow rate of 22 mL/h. The column was equilibrated with PBS7.4. A gel filtration calibration kit (Pharmacia) including hemoglobin (R_s = 31 Å), bovine serum albumin (R_s = 37 Å), catalase (R_s = 52 Å), ferritin (R_s = 60 Å), and thyroglobulin (R_s = 81 Å) was used to calibrate the column. The R_s values of these proteins were given with the literature accompanying the kit. Dextran blue was used to calculate the void volume (V_o). The partition coefficient (K_{av}^x) of protein x was calculated according to the equation:

$$K_{av}^{x} = (V_e^x - V_o)/(V_t - V_o)$$

where V_e^x = the elution volume of protein x and V_t = the total volume of the column. A linear calibration curve ($\log R_s = 2.52 - 1.22K_{av}$) was obtained for the proteins in the kit and was used to calculate the R_s of spectrin under different ionic strengths. The K_{av} values of spectrin in 5P7.4 with different NaCl concentrations were obtained with the column pre-equilibrated with the appropriate buffer. The R_s values calculated from K_{av} values for spectrin dimers were 124 ± 5 (n = 2), 155, 160, and 178 Å for 5P7.4 buffer containing 150, 100, 50, and 0 mM NaCl, respectively. Although the R_s values calculated for the spectrin dimer were considerably larger than those of the calibration proteins, previous work using similar calibration proteins has shown that this treatment is reliable for spectrin (Kam *et al.*, 1977). The R_s values under different ionic strengths are in good agreement with those published earlier (Schmidt *et al.*, 1993; Elgsaeter, 1978) showing changes of Stokes radii as a function of ionic strength. Thus, we have shown that the spectrin samples used in this study do exhibit the reported changes in the hydrodynamic property induced by ionic strength.

Electronic Circular Dichroism Spectroscopy. Electronic CD (ECD, commonly called CD) spectra were obtained with

[1] Abbreviations: 0.3P7.6, 0.3 mM sodium phosphate buffer at pH 7.6; 5P7.4, 5 mM sodium phosphate buffer at pH 7.4; 5P8, 5 mM sodium phosphate buffer at pH 8.0; ECD, electronic circular dichroism; EPR, electron paramagnetic resonance; FSD, Fourier self-deconvolution; FTIR, Fourier transform infrared; FWHH, full width at half-height; K_{av}, partition coefficient; NMR, nuclear magnetic resonance; PBS7.4, 5 mM sodium phosphate buffer with 150 mM NaCl at pH 7.4; PBS8, 5 mM sodium phosphate buffer with 150 mM NaCl at pH 8.0; PLS, partial least squares; RBCs, red blood cells; R_s, Stokes radius; SDS, sodium dodecyl sulfate; SUBH2O, buffer subtraction program; TGS, triglycine sulfate; VCD, vibrational circular dichroism; V_e, elution volume; V_o, void volume; V_t, total column volume.

a JASCO J-600 CD instrument over the range of 180–260 nm, under conditions similar to those reported previously (Pancoska & Keiderling, 1991). Briefly, spectrin (0.70–0.73 mg/mL, as calculated from the molar absorptivity reported above) in PBS7.4 or 5P7.4 buffer was placed in a 0.1-mm quartz cell at room temperature, and spectra were scanned with a 1-nm band-pass at a 2-s time constant. The photomultiplier high voltage became excessively high at 182 nm for the low-salt sample and at 192 nm for the high-salt sample. Base-line correction was done with the standard software by subtraction of a ECD buffer blank. An initial estimate of the percentage of α-helix was obtained from the mean residue ellipticity at 222 nm (Chen & Yang, 1971).

Vibrational Circular Dichroism Spectroscopy. Vibrational CD (VCD) spectra were obtained on a dispersive instrument that has been described in detail previously (Keiderling, 1990). A resolution of $\sim$10 cm^{-1} in the region of 1750–1550 cm^{-1} was used. The spectra were collected with a 10-s time constant and are the average of 4 scans. The spectrin dimer sample (500 μL at 35 $\pm$ 5 mg/mL) was subjected to D_2O exchanges 4 times, by concentrating samples in microconcentrators (Amicon), followed by dilution with about 1.5 mL of PBS7.4 buffer prepared with D_2O (99.9%; Norell, Inc., Landisville, NJ) each time. The D_2O-exchanged sample was further concentrated to a very viscous solution with an estimated final concentration of about 60 mg/mL. The filtrate from the last exchange was saved and used in the VCD measurements to give a background spectrum of the residual HOD/H_2O in the sample. The sample was then placed into a home-built cell composed of CaF_2 windows (2 $\times$ 25 mm) separated by a 25-μm Teflon spacer. The same sample was also scanned on a Digilab FTS-40 (Bio-Rad) FTIR spectrometer as a check of the dispersive result (data not shown). The center frequency of the amide I band in D_2O (amide I') from the second derivative of the FTIR absorbance spectrum was 1647 cm^{-1}, which is a 4-cm^{-1} shift from the center frequency of the corresponding band in H_2O (see below), as expected.

FTIR Spectroscopy. A Bio-Rad FTS-40 FTIR spectrophotometer with a triglycine sulfate (TGS) detector was used to record the FTIR spectra, as has been described (Pancoska *et al.*, 1993). Typically, 1024 interferograms were recorded at 20 °C, co-added, and Fourier-transformed with triangular apodization at a nominal resolution of 2 cm^{-1}. For the measurements of samples in H_2O buffer, a semi-permanent cell equipped with CaF_2 salt plates and a 6-μm tin spacer was used. The 6-μm spacer kept the 1640-cm^{-1} H_2O absorbance below 1 and permitted quantitative spectral subtraction of the background (Dousseau & Pezolet, 1990). An open aperture was used to allow the maximum light level to reach the detector, which should not have a negative impact on resolution in this spectral region. For each run, a single-beam spectrum was collected on the spectrin sample, the buffer (background), and a clean empty cell (air).

FTIR Data Analysis. (A) Water Absorption Correction. The absorbance spectra of the samples and of the buffer were determined from the single-beam intensity spectra referenced to air. The buffer absorbance spectrum was subtracted from the spectrin absorbance spectrum to give the absorbance spectrum of spectrin in buffer. Three spectral subtraction methods were used. Two of the subtractions were performed manually, using both the Digilab and the Spectra Calc (Galactic Industries, Salem, NH) software, and one subtraction was done with the automatic method using an array basic program (SUBH20) (Dousseau *et al.*, 1989), which was written in Spectra-Calc software and was generously provided to us by Professor M. Pezolet of Laval University. Two spectral subtraction criteria were followed, namely, to obtain a flat base line in the region from 2000 to 1750 cm^{-1} (Dong *et al.*, 1990) and to achieve the most narrow amide I band.

(B) Secondary Structure Analysis. The absorbance spectra of spectrin in buffer corrected for water absorption (the subtracted spectra) were then analyzed by two independent methods to provide information on the secondary structure of spectrin. The first method was the band-fitting approach (Byler & Susi, 1986), which assumes that the integrated area under a curve-fitted band is proportional to the concentration of secondary structure responsible for that band. Band assignment to α-helix was made according to the literature (Byler & Susi, 1986; Susi & Byler, 1986; Holloway & Mantsch, 1989; Dong *et al.*, 1990; Venyaminov & Kalnin, 1990). The positions of the bands were determined from the second-derivative spectra of the subtracted spectra. Fourier self-deconvolution (FSD) (Kauppinen *et al.*, 1981) of the subtracted spectra was carried out, using a triangular apodization function with a resolution enhancement parameter of $K = 2.0$ and a full width at half-height parameter (FWHH) of 14 cm^{-1}. These parameters assured that the spectra were not overdeconvolved as was evidenced by the absence of negative side lobes. The Digilab software was used for obtaining both the second-derivative spectra and the FSD spectra. The band-shape fitting was then performed on the deconvolved spectra, assuming a 100% Gaussian band shape and using the band-fit routine in the Spectra–Calc software.

The second method was the partial least-squares (PLS) analysis method (Dousseau & Pezolet, 1990). Fourteen spectra of proteins of H_2O buffer with known secondary structures, obtained from Professor M. Pezolet, were used as the original training set, and were input into the PLS QUANT module of Spectra-Calc, and a PLS calibration spectrum was calculated using a dimension of 25 and 4 components (ordered α-helix, unordered α-helix, β-sheet, and other, which includes turns and random coil). One of the training set proteins in polylysine at high pH which was assumed to have 100% α-helix. Since polylysine is sometimes unstable under these conditions, the calibration spectra were recalculated without this polypeptide. However, there was no significant difference in the structural predictions made without polylysine, so it was left in the training set for the final analysis. The overall intensities of the absorbance spectra of corrected for water absorption (subtracted spectra) were normalized to unity (Dousseau & Pezolet, 1990) before analysis with the PLS method. For comparison to the band-fitting results, the ordered and unordered helix components of spectrin were added together and presented as the total α-helix content.

RESULTS

ECD Spectra of Spectrin. Upon visual inspection, the spectra (not shown) in both high-salt (PBS7.4) and low-salt (5P7.4) buffers resemble the published spectra on spectrin (Ralston, 1978). The high-salt buffer with 150 mM NaCl prevented us from obtaining the ECD spectra down to 180 nm. Thus, we were not able to use the most reliable, quantitative analyses based on full band shape single variable decomposition (Hennessey & Johnson, 1981) or our own principle component method for factor analysis (Pancoska & Keiderling, 1991) to analyze the ECD spectra of spectrin in PBS7.4. This makes it difficult to use ECD to provide a quantitative comparison of spectrin in high-salt and low-salt environments. As an indication of the helix content, the mean residue ellipticity at 222 nm was used to estimate the α-helix

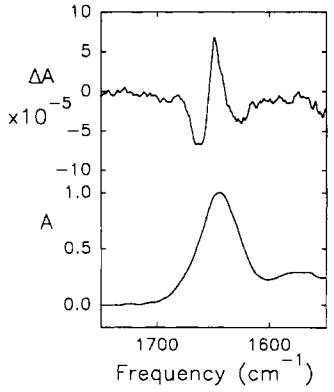

FIGURE 1: VCD and dispersive IR spectra of spectrin (estimated to be 60 mg/mL) in PBS7.4/D_2O. A resolution of ~10 cm^{-1} in the region of 1750–1550 cm^{-1} was used. The spectra were collected with a 10-s time constant and are the average of 4 scans. The filtrate from the last D_2O exchange was saved and used in the VCD measurements to give a background spectrum of the residual HOD/H_2O in the sample.

fraction (Chen & Yang, 1971; Johnson, 1988). The values of 77% α-helix for spectrin in PBS7.4 (high salt) and 75% for spectrin in 5P7.4 (low salt) were obtained.

VCD Spectra of Spectrin. Figure 1 shows the VCD and dispersive IR spectra of spectrin in PBS7.4/D_2O. The VCD spectrum is consistent in shape and magnitude with that of a very highly α-helical protein. However, the absorbance maximum determined from the FTIR absorbance spectrum of spectrin in D_2O (1647 cm^{-1}) and consequently the main VCD features are significantly lower in frequency than for typical globular proteins such as hemoglobin in D_2O (1651 cm^{-1}) (see below). Consequently, use of our factor analysis methods for quantitative study of proteins VCD (Pancoska & Keiderling, 1991) leads to unreliable values.

Secondary Structure of Spectrin in High-Salt Buffer. A typical FTIR absorbance spectrum of spectrin dimer (35 ± 5 mg/mL) in PBS7.4 is shown in Figure 2a. The spectrum had two major bands. The band in the 1700–1600-cm^{-1} region was assigned to the amide I transition and the band in the 1600–1500-cm^{-1} region to the amide II transitions. The amide I band was relatively more symmetric and narrow than other proteins with low helix contents (Dousseau & Pezolet, 1990), which is consistent with a protein of high α-helix content.

The second-derivative spectrum of the absorbance spectrum (Figure 2b) indicated that the amide I band was comprised of three major components at 1681, 1651, and 1631 cm^{-1}. The largest peak at 1651 cm^{-1} was assigned to the α-helix component.

The FSD spectrum in Figure 2c revealed that band narrowing by the deconvolution operation allowed the decomposition of the amide I band into its underlying components. This FSD spectrum was band-fitted down to 1500 cm^{-1} (Figure 2d) to ensure minimum error due to overlap between the amide I and II regions. However, for quantitation of the secondary structure, our attention was focused on the amide I region only, which gave rise to five bands. The band centered at 1651 cm^{-1} was assigned to the α-helix, as mentioned above, and accounted for 55% of the integrated intensity as judged from our "best" fit (see below). Other bands were very difficult to assign uniquely (Pancoska *et al.*, 1993) and for that reason will not be discussed further. The Byler and Susi band-fit approach to the analysis of protein FSD-FTIR assumes that the extinction coefficient for each secondary structural type is the same so that the relative areas under the component bands are proprotional to the fraction of that

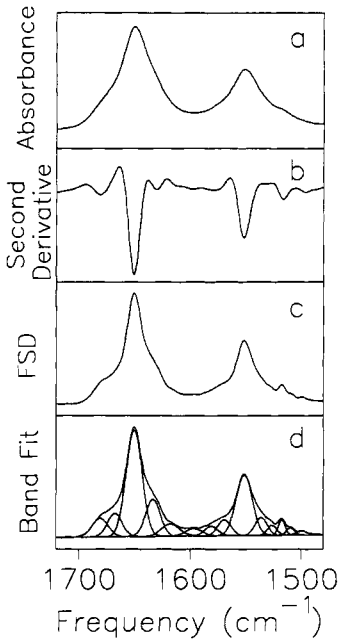

FIGURE 2: FTIR absorbance, second-derivative, FSD deconvolution, and band-fitted spectra of spectrin (35 ± 5 mg/mL) in PBS7.4 buffer. (a) Absorbance spectrum (resolution 2 cm^{-1}). (b) Second-derivative spectrum of the absorbance spectrum in (a). (c) Deconvolved spectrum of the absorbance spectrum in (a) using deconvolution parameters FWHH = 14 cm^{-1} and K = 2. (d) Band-fit of the deconvolved spectrum from (c). The spectrum was band-fitted down to 1500 cm^{-1} to ensure minimum error due to overlap between the amide I and II regions. The five bands in the amide I region yield 55% α-helix.

secondary structure type in the protein (Byler & Susi, 1986). However, because our absorbance spectrum was not over-deconvolved, the variance in the band shape was not sufficient to constrain this multiparameter fit to a unique solution. We found that the percentage of α-helix obtained with this method varied from 45 to 60% depending on the constraints to the fit and the initial peak parameters used. Therefore, the band-fit method was determined to be unreliable for our purposes.

Although band-fitting provides a basis for the quantitative estimation of the secondary structure of proteins, it is not a routine procedure since there was difficulties with obtaining artifact-free resolution-enhanced spectra with the band-fitting procedure (Dousseau & Pezolet, 1990). By contrast, the PLS method of spectral analysis is a more robust technique. Due to the objectivity and relative ease of the PLS method of analysis, all the spectra of the modified spectrin in buffer samples were analyzed with the PLS method. Analysis of a typical FTIR absorbance spectrum of spectrin in PBS7.4 (Figure 2a) yields 67% α-helix, 10% β-sheet, and 23% other. The average values of four runs showed that spectrin consisted of about 70% α-helix, 10% β-sheet, and 20% other (Table I). These values are presumably reliable to within 5–6% (Dousseau & Pezolet, 1990).

We used three different methods to correct the absorbance spectra for H_2O absorption, as outlined under Materials and Methods, to assess their effect on the PLS analysis. The resultant intensity of the amide I band in the subtracted spectra varied by as much as 14%, while the intensity of the amide II band was constant regardless of the subtraction method. The overall intensities of the subtracted spectra were normalized to unity, as indicated under Materials and Methods. This normalization led to the equalization of the amide I intensity, and a variation of about 14% in the amide II band intensity. However, these changes in the band intensities did

Table I: Secondary Structure Components from PLS-Analyzed Spectra of Spectrin Dimer and Modified Spectrin in 5 mM Phosphate Buffer at pH 7.4 (5P7.4) and in 5 mM Phosphate Buffer with 150 mM NaCl at pH 7.4 (PBS7.4) at 20 °C

	PBS7.4	PBS7.4 + 2 M NaOH	PBS7.4 + 1% SDS	5P7.4
% α-helix	69 ± 5[a] (n = 4)[b]	51 ± 9[c] (n = 2)	51 ± 2 (n = 2)	74 ± 6 (n = 2)
% β-sheet	10 ± 4	16 ± 4	16 ± 1	12 ± 3
% other	21 ± 4	34 ± 5	33 ± 1	14 ± 9

[a] Error denotes the standard deviation of multiple runs. [b] n is the number of experiments. [c] Error denotes the difference of two runs.

not significantly affect the results of the PLS analysis. The α-helix contents remained similar while the predicted β-sheet and other components varied by up to 2%. Thus, PLS analysis results were independent of the method used for spectral subtraction, and the automatic method (Pezolet subtraction) was used routinely.

Sensitivity of FTIR to Secondary Structural Changes in Spectrin. The FTIR data of spectrin at high pH (2 M NaOH) and of SDS-treated spectrin were also obtained (Table I). The results were similar in both systems. The α-helix content decreased about 20% (from 70% to 50%). The β-sheet content increased slightly. The structural components defined as other increased to about 35%. Thus, the FTIR absorbance spectra are sensitive to the secondary structural changes in spectrin induced by denaturants, and the values determined show sensible changes from the results for the native form.

Secondary Structure of Spectrin in Low-Salt Buffer. The FTIR spectra of spectrin in 5P7.4 were very similar to those of spectrin in high-salt buffer. The average values of the PLS analysis of two different runs were 74% α-helix, 12% β-sheet, and 14% other (Table I). These values were very similar to those for spectrin in high-salt buffer (PBS7.4) (69% α-helix, 10% β-sheet, and 21% other).

Center Frequency of the Major Component in Amide I. The center frequency of the main component of the amide I band assigned to the α-helix of spectrin was examined under different experimental conditions. This frequency for spectrin in PBS7.4 was 1651 cm^{-1} (n = 5) and remained unchanged in 5P7.4 (1651 cm^{-1}, n = 3). However, SDS treatment caused a frequency upshift of 3 cm^{-1} (1654 cm^{-1}, n = 2), and NaOH treatment caused a frequency upshift of 1 cm^{-1} (1652 cm^{-1}, n = 2).

DISCUSSION

In this study, we obtained reliable ECD, VCD, and FTIR spectra of erythrocyte spectrin in high-salt (PBS7.4) and in low-salt (5P7.4) buffers at room temperature. We observed no detectable difference in spectral features under these two ionic strength conditions. PLS analysis of the FTIR data shows about 70% α-helix, 10% β-sheet, and 20% other for spectrin in both buffers. The uncertainties in these values are about 5–6%.

All spectroscopic determinations of secondary structure are subject to considerable absolute error, but may prove very useful for monitoring relative changes, if any, as sought here. To improve the structural interpretation made, multiple techniques should be employed. The reliability and limits of using the multiple techniques ECD, VCD, and FTIR for the determination of secondary structure have been thoroughly discussed in review articles (Keiderling & Pancoska, 1993; Surewicz *et al.*, 1993; Sarver & Kreuger, 1991). In this study of human erythrocyte spectrin, we have collected the ECD and VCD spectra to complement the FTIR data. However, problems were encountered in carrying out quantitative analysis of the ECD and VCD spectra of spectrin in PBS7.4. Although both the ECD and VCD spectra of spectrin have band shape characteristics of a highly α-helical protein, accurate quantitative analyses were not possible for either the ECD spectra, due to the large chloride ion absorbance interference at lower wavelengths (<210 nm), or the VCD spectra, due to a frequency shift. However, from the mean residue ellipticity at 222 nm in the ECD spectra, the α-helical content for spectrin can be estimated to be about 77% in PBS7.4 and 75% in 5P7.4, which are in agreement with the earlier ECD value of 65–70% (Ralston, 1978; DeVogel *et al.*, 1979; Calvert *et al.*, 1980). The VCD band shape was a good match with those of other highly helical proteins, and its intensity was at least as high as that of hemoglobin. The actual values obtained for spectrin from a quantitative analysis of the VCD were higher than for hemoglobin, but we believe that this high value could be an artifact due to the frequency shift. At any rate, values above ~70% helical are suspect in our analyses due to lack of reference spectra in our training set representing proteins of higher helical content.

FTIR spectroscopic methods have an advantage over conventional ECD methods in the prediction of small percentages of β-sheet (Sarver & Kreuger, 1991) due to the resolved nature of the vibrational bands. Furthermore, solvent interference (such as chloride ions) is not a problem in the FTIR spectrum. Difficulties in the assignment of the deconvoluted bands may arise due to noise, water vapor, amino acid side chains, or contaminants (Lee *et al.*, 1990). In addition, the nonuniqueness of the absorption bands could cause inappropriate assignments (Pancoska *et al.*, 1993; Surewicz *et al.*, 1993). Recent reviews have addressed the potential problems of quantitative analysis of the secondary structure of proteins from FTIR spectra (Arrondo *et al.*, 1993; Surewicz *et al.*, 1993). Careful base-line correction and water vapor subtraction must be carried out in order to yield an artifact-free spectrum. An awareness and avoidance of the potential problems can increase the reliability of secondary structure predictions made from FTIR spectra of proteins. Therefore, as a precaution in our analysis of the secondary structure of spectrin in H_2O buffer, we used two different techniques: the band-fitting of the FSD deconvoled amide I region and partial least-squares (PLS) analysis of amide I and amide II regions. It is reassuring that the two data analysis techniques (PLS and band-fitting) yielded similar secondary structural information for spectrin in PBS7.4. Specifically, using PLS analysis, the secondary structure coponents of spectrin dimers in PBS7.4 were about 70% α-helix, 10% β-sheet, and 20% other. Our optimal band-fitting of the FSD deconvolved absorbance spectrum of spectrin (done before the PLS analysis and thus not biased by these results) gave 55% α-helix. Since the potential error was less for the PLS analysis method than the band-fitting method, we used the more objective PLS method for the majority of our analyses. Unlike for the quantitative VCD analysis, the PLS secondary structure predictions appear to be relatively insensitive to the shift of the main α-helical feature to lower frequency (see discussions below). This insensitivity is evidenced in one sense by the close parallel of the band shape fitting result (both qualitatively and quantitatively) and the PLS prediction. Presumably, this ability to encompass a substantial frequency shift in the major component is due to the low-resolution character of the data being analyzed and to the ability to encompass both the amide I and the amide II data in a single

analysis. In addition, using two types of helix—ordered and disordered—to account for the frequency shift improves the helix prediction to about 6% (Dousseau & Pezolet, 1990). Our preliminary work on factor analysis shows improved qualitative prediction when amide II VCD data are included (Pancoska *et al.*, unpublished results), but the frequency position sensitivity of VCD analyses must be a function of its differential band shape leading to an intrinsically higher resolution definition of the spectrum as compared to undeconvolved FTIR.

It is interesting to note that our PLS analysis suggests, for the first time, significant (about 10%) β-sheet in spectrin. Future structural modeling studies of the spectrin conformation should include this structural feature. A recent publication on the structure of the 62 amino acid SH3 domain in the center of spectrin shows 5 antiparallel β-strands (Musacchio *et al.*, 1992; Yu *et al.*, 1992). The amino acids in this domain account for only about 1.5% of the total amino acid residues in the spectrin dimer. Thus, these data suggest that either other nonrepeating regions in spectrin are substantially β-sheet or that the 106-repeating units include more β-sheet structure than has been considered to date. More detailed studies of spectrin monomers and of different spectrin subfragments may provide information on the location of β-sheet structure in spectrin.

The secondary structural changes detected by FTIR on spectrin treated with 2 M NaOH or 1% SDS demonstrate the sensitivity of the FTIR methods to structural changes in spectrin. The data show that these treatments cause a decrease in α-helix content by about 20%, while the other structural components increased from about 20% to 35%. Gel filtration chromatography has shown that SDS treatment causes the spectrin molecule to unfold (Nozaki *et al.*, 1976). However, no change in the content of α-helix, β-sheet, or other was found in spectrin when the salt concentration of the medium was decreased from 150 to 0 mM, despite the Stokes radius variation from 124 Å in PBS7.4 to 178 Å in 5P7.4.

The frequency shifts of the major component in the amide I band of highly α-helical proteins (discussed above) can be used independently to report on the changes in hydrogen bond strength within the helices. For example, the frequency shifts observed in different proteins under the same experimental conditions (Dousseau *et al.*, 1990) or in one protein under different experimental conditions (George & Veiss, 1991; Zhang *et al.*, 1992) have been correlated with changes in helical lengths due to changes in hydrogen bond strength in highly helical proteins. For proteins of high α-helical content under similar experimental conditions, a protein with low amide I band frequency has a large fraction of ordered helix as compared to disordered helix and thus a long helical length. This frequency shift has been correlated to the difference in hydrogen bonding of the amide groups at the end of helical segments (disordered helix) compared to those in the center (order helix) (Van Wart & Scheraga, 1978). Many model α-helical polypeptides of long coherence length also have low-frequency amide I bands (Parker, 1971). It is interesting to note here that the center frequency for spectrin at 1651 cm^{-1} is lower than that for hemoglobin (1654 cm^{-1}) (Dong *et al.*, 1990; Susi & Ryler, 1986) and higher than that for tropomyosin (1643 cm^{-1}) (Dousseau *et al.*, 1990). While this difference between spectrin and hemoglobin is small, it suggests that spectrin consists of helices longer than those in hemoglobin. The data also suggest that the spectrin helices are shorter than those in tropomyosin. Undoubtedly, the coiled-coil structure of tropomyosin could cause a frequency shift to lower frequency. For one protein under different experimental conditions, the conditions to give low frequency corresponds to a long helical length in protein under that condition. For example, the 1660-cm^{-1} band in the spectrum of intact collagen was attributed to proline residues in the collagen helix which form very weak hydrogen bonds, and the frequency was shifted to 1630 cm^{-1} upon melting of collagen to give stronger hydrogen bonds (George & Veiss, 1991). In addition, peptide conformational changes due to mismatch of peptide hydrophobic length and bilayer hydrophobic thickness also produce frequency shifts (Zhang *et al.*, 1992). For spectrin, when comparing the amide I center peak frequency of the spectra in high- and low-salt buffer, no frequency shift was observed and the frequency remained at 1651 cm^{-1}, indicating no change in hydrogen bond strength and thus no change in helical segment length in spectrin. By contrast, spectrin under denaturing conditions exhibits a distinct center frequency shift, to higher frequency. These shifts to higher frequencies are consistent with weaker hydrogen bonding and a larger fraction of disordered helix in the denatured protein.

Earlier experiments, based on ORD measurements and using similar buffer systems as we used, yielded no difference in the secondary structure of the dimer with values of 58% α-helix in buffer with 100 mM NaCl and 54% in buffer with no NaCl (Ralston & Dunbar, 1979). ECD experiments revealed that the α-helical content of spectrin tetramer decreases slightly (3%) when the ionic strength is lowered (Ralston & Dunbar, 1979), but this change is well within the error limits of the ECD technique.

Our ECD, VCD, and FTIR data indicate no salt-induced changes in the secondary structural content or α-helical length in spectrin beyond our error limits. Therefore, the salt-induced hydrodynamic (Ralston, 1976; Brauer *et al.*, 1977; Ralston & Dunbar, 1979; Elgasaeter, 1978) and molecular dynamic (our unpublished NMR and EPR results) changes observed before cannot be attributed to secondary structural changes, neither in content nor in α-helical length.

In the coiled-coil model of spectrin, the helices are stablized relative to one another by charge–charge interactions among amino acids arranged in a heptad pattern along a vertical axis (Parry *et al.*, 1992). It is possible that the helices may change their register with each other to favor different sets of charge–charge interactions resulting in tertiary structural transformation under different ionic strengths. It is also possible that spectrin does not undergo either secondary or tertiary structural transformation under different salt conditions. It has been suggested that the α- and β-subunits are twisted about a common axis, forming a two-start helix with 2-fold rotational symmetry, and the elastic deformation of the erythrocyte is mediated by transient extension of the helix (McGough & Josephs, 1990). Some of the observed salt-induced changes may be due to conformational changes related to dimer to tetramer conversions. It has been reported that the equilibrium of dimers and tetramers is strongly dependent on ionic strength, favoring dimers at low salt concentrations and tetramers at physiological and higher salt concentrations (Ungewickell & Gratzer, 1978). It has also been reported that charge–charge interactions stabilize the tetramer, and when the ionic strength of the medium is decreased below 0.05 M, dissociation to heterodimers is enhanced (Cole & Ralston, 1992). Further studies of spectrin by techniques that are able to distinguish dimer and tetramer entities, such as dynamic light scattering, and studies of spectrin subfragments may provide information on the molecular origin of the salt-induced changes reported in the literature.

ACKNOWLEDGMENT

We acknowledge Professor M. Pezolet of Laval University for the SUBH2O program, for the protein spectra for the training set, and for helpful discussions.

REFERENCES

Arrondo, J. L. R., Muga, A., Castreasana, J., & Goni, F. M. (1993) *Prog. Biophys. Mol. Biol. 59*, 23–56.
Brauer, E., Kupka, K.-D., & Rudloff, V. (1977) *Bioelectrochem. Bioenerg. 5*, 223–231.
Budzynski, D. M., Benight, A. S., LaBrake, C. C., & Fung, L. W.-M. (1992) *Biochemistry 31*, 3653–3660.
Byler, D. M., & Susi, H. (1986) *Biopolymers 25*, 469–487.
Calvert, R. P., Bennett, V., & Gratzer, W. (1980) *Eur. J. Biochem. 107*, 355–361.
Chen, Y.-H., & Yang, J. T. (1971) *Biochem. Biophys. Res. Commun. 44*, 1285–1291.
Clague, M. J., Harrison, J. P., Morrision, I. E. G., Wyatt, K. J., & Cherry, A. J. (1990) *Biochemistry 29*, 3898–3904.
Clarke, M. (1971) *Biochem. Biophys. Res. Commun. 45*, 1063–1070.
Cole, N., & Ralston, G. B. (1992) *Biochim. Biophys. Acta 1121*, 23–30.
Davison, M. D., Baron, M. D., & Critchley, D. R., & Wootton, J. C. (1989) *Int. J. Biol. Macromol. 11*, 81–90.
DeVogel, M., Leonis, J., Noyer, M., Polastro, E., Schnek, A. G., & Vincentelli, J. (1979) *Reun. D'Anver 1*, 1036–1037.
Dong, A., Huang, P., & Caughey, W. S. (1990) *Biochemistry 29*, 3303–3308.
Dousseau, F., & Pezolet, M. (1990) *Biochemistry 29*, 8771–8779.
Dousseau, F., Therrien, M., & Pezolet, M. (1989) *Appl. Spectrosc. 43*, 538–542.
Dubreuil, R. R., Byers, T. J., Stillman, A. L., Bar-Zvi, L. S., Goldstein, B., & Branton, D. (1989) *J. Cell Biol. 109*, 2197–2205.
Elgsaeter, A. (1978) *Biochim. Biophys. Acta 536*, 235–244.
Fung, L. W.-M., & Johnson, M. E. (1983) *J. Magn. Reson. 51*, 233–244.
Fung, L. W.-M., Lu, H.-A., Hjelm, R. P., Jr., & Johnson, M. E. (1986) *FEBS Lett. 105*, 379–383.
Fung, L. W.-M., Lu, H.-A., Hjelm, R. P., Jr., & Johnson, M. E. (1989) *Life Sci. 44*, 735–740.
George, A., & Veiss, A. (1991) *Biochemistry 30*, 2372–2377.
Hennessey, J. P., Jr., & Johnson, W. C., Jr. (1981) *Biochemistry 20*, 1085–1094.
Holloway, P. W., & Mantsch, H. H. (1989) *Biochemistry 28*, 931–935.
Johnson, R. M., Taylor, G., & Meyer, D. B. (1980) *J. Cell Biol. 86*, 371–376.
Johnson, W. C., Jr. (1988) *Annu. Rev. Biophys. Biophys. Chem. 17*, 145–166.
Kam, Z., Josephs, R., Eisenberg, H., & Gratzer, W. B. (1977) *Biochemistry 16*, 5568–5572.
Kauppinen, J. K., Moffatt, D. J., Mantsch, H. H., & Cameron, D. G. (1981) *Appl. Spectrosc. 35*, 271–276.
Keiderling, T. A. (1990) *Practical Fourier Transform Spectroscopy* (Ferraro, J. R., & Krisham, K., Eds.) pp 203–284, Academic Press, New York.
Keiderling, T. A., & Pancoska, P. (1993) in *Advances in Spectroscopy* (Clark, R. J. H., & Hester, R. E., Eds.) Part B, pp 267–315, John Wiley & Sons, Chichester, U.K.
Lange, Y., Hadesman, R. A., & Steck, T. L. (1982) *J. Cell Biol. 92*, 714.
Lee, D. C., Haris, P. I., Chapman, D., & Mitchell, R. C. (1990) *Biochemistry 29*, 9185–9193.
Marchesi, S. L., Steers, E., Marchesi, V. T., & Tillach, W. T. (1969) *Biochemistry 9*, 50–57.
McGough, A. M., & Josephs, R. (1990) *Proc. Natl. Acad. Sci. U.S.A. 87*, 5208–5212.
Mikkelsen, A., & Elgsaeter, A. (1978) *Biochim. Biophys. Acta 536*, 245–251.
Mikkelsen, A., Stokke, B. T., & Elgsaeter, A. (1984) *Biochim. Biophys. Acta 786*, 95–102.
Musacchio, A., Noble, M., Pauptit, R., & Saraste, M. (1992) *Nature 359*, 851–855.
Nozaki, Y., Schecter, N. M., Reynolds, J. A., & Tanford, C. (1976) *Biochemistry 15*, 3884–3890.
Pancoska, P., & Keiderling, T. A. (1991) *Biochemistry 30*, 6885–6895.
Pancoska, P., Wang, L., & Keiderling, T. A. (1993) *Protein Sci. 2*, 411–419.
Parker, F. S. (1971) *Applications of Infrared Spectroscopy in Biochemistry, Biology & Medicine*, Plenum Press, New York.
Parry, D. A. D., Dixon, T. W., & Cohen, C. (1992) *Biophys. J. 61*, 858–867.
Ralston, G. B. (1976) *Biochim. Biophys. Acta 443*, 387–393.
Ralston, G. B. (1978) *J. Supramol. Struct. 8*, 361–373.
Ralston, G. B., & Dunbar, J. C. (1979) *Biochim. Biophys. Acta 579*, 20–30.
Sahr, D. E., Laurila, P., Kotula, L., Scarpa, A. L., Coupal, E., Leto, T. L., Linnenbach, A. J., Winkelmann, J. C., Speicher, D. S., Marchesi, V. T., Curtis, P. J., & Forget, B. G. (1990) *J. Biol. Chem. 265*, 4434–4443.
Sarver, R. W., Jr., & Kreuger, W. C. (1991) *Anal. Biochem. 194*, 89–100.
Schmidt, C. F., Svoboda, K., Lei, N., Petsche, I. B., Berman, L. E., Safinya, C. R., & Grest, G. S. (1993) *Science 259*, 952–955.
Shotton, D. M., Burke, B. E., & Brank, D. (1979) *J. Mol. Biol. 131*, 303–329.
Speicher, D. V., Gary, D., & Marchesi, V. T. (1983) *J. Biol. Chem. 258*, 15938–15947.
Speicher, D. V., Weglarz, L., & DeSilva, T. M. (1992) *J. Biol. Chem. 267*, 14775–14782.
Speicher, D. V., DeSilva, T. M., Speicher, K. D., Ursitti, K. D., Ursitti, J. A., Hembach, P., & Weglarz, L. (1993) *J. Biol. Chem. 268*, 4227–4235.
Surewicz, W. K., & Mantsch, H. H. (1988) *Biochim. Biophys. Acta 952*, 115–130.
Surewicz, W. K., Mantsch, H. H., & Chapman, D. (1993) *Biochemistry 32*, 389–394.
Susi, H., & Byler, D. M. (1986) *Methods Enzymol. 130*, 390.
Svoboda, K., Schmidt, C. F., Branton, D., & Block, S. M. (1992) *Biophys. J. 63*, 784–793.
Ungewickell, E., & Gratzer, W. (1978) *Eur. J. Biochem. 88*, 379–385.
Van Wart, H. E., & Scheraga, H. A. (1978) *Methods Enzymol. 49*, 67–149.
Venyaminov, S. Y., & Kalnin, N. N. (1990) *Biopolymers 20*, 1259–1271.
Vertessy, B. G., & Steck, T. L. (1989) *Biophys. J. 55*, 255–262.
Winkelmann, J. C., Leto, T. L., Watkins, P. C., Eddy, R., Shows, T. B., Linnenbach, A. J., Sahr, K. E., Kathuria, N., Marchesi, V. T., & Forget, B. T. (1988) *Blood 72*, 328–334.
Winkelmann, J. C., Chang, J.-G., Tse, W. T., Scarpa, A. L., Marchesi, V. T., & Forget, B. G. (1990) *J. Biol. Chem. 265*, 11827–11832.
Xu, Y., Prabhakaran, M., Johnson, M. E., & Fung, L. W.-M. (1990) *J. Biomol. Struct. Dyn. 8*, 55–62.
Yu, H., Rosen, M. K., Shin, T. B., Seidal-Dugan, C., Brugge, J. S., & Schreiber, S. L. (1992) *Science 258*, 1665–1668.
Zhang, Y.-P., Lewis, R. N. A. H., Hodges, R. S., & McElhaney, R. N. (1992) *Biochemistry 31*, 11579–11588.